

RESEARCH/REVIEW ARTICLE

Transpression and tectonic exhumation in the Heimefrontfjella, western orogenic front of the East African/Antarctic Orogen, revealed by quartz textures of high strain domains

Wilfried Bauer,^{1,2} Heinrich Siemes,¹ Gerhard Spaeth¹ & Joachim Jacobs^{3,4}¹ Energy & Mineral Resources Group, RWTH Aachen University, Wüllnerstr. 2, DE-52056 Aachen, Germany² Department of Applied Geosciences, German University of Technology in Oman, PO Box 1816, 130 Athaibah, Sultanate of Oman³ Department of Earth Science, University of Bergen, Allegaten 41, NO-5007 Bergen, Norway⁴ Norwegian Polar Institute, Fram Centre, PO Box Langnes, NO-9296 Tromsø, Norway**Keywords**

Dronning Maud Land; quartz microfabrics; X-ray texture goniometry; shear zones; mylonites.

CorrespondenceWilfried Bauer, Department of Applied Geosciences, German University of Technology in Oman, PO Box 1816, 130 Athaibah, Sultanate of Oman.
E-mail: bauer@geol.rwth-aachen.de**Abstract**

The metamorphic basement of the Heimefrontfjella in western Dronning Maud Land (Antarctica) forms the western margin of the major ca. 500 million year old East African/East Antarctic Orogen that resulted from the collision of East Antarctica and greater India with the African cratons. The boundary between the tectonothermally overprinted part of the orogen and its north-western foreland is marked by the subvertical Heimefront Shear Zone. North-west of the Heimefront Shear Zone, numerous low-angle dipping ductile thrust zones cut through the Mesoproterozoic basement. Petrographic studies, optical quartz c-axis analyses and x-ray texture goniometry of quartz-rich mylonites were used to reveal the conditions that prevailed during the deformation. Mineral assemblages in thrust mylonites show that they were formed under greenschist-facies conditions. Quartz microstructures are characteristic of the subgrain rotation regime and oblique quartz lattice preferred orientations are typical of simple shear-dominated deformation. In contrast, in the Heimefront Shear Zone, quartz textures indicate mainly flattening strain with a minor dextral rotational component. These quartz microstructures and lattice preferred orientations show signs of post-tectonic annealing following the tectonic exhumation. The spatial relation between the sub-vertical Heimefront Shear Zone and the low-angle thrusts can be explained as being the result of strain partitioning during transpressive deformation. The pure-shear component with a weak dextral strike-slip was accommodated by the Heimefront Shear Zone, whereas the north–north-west directed thrusts accommodate the simple shear component with a tectonic transport towards the foreland of the orogen.

To access the supplementary material for this article, please see the supplementary file under Article Tools, online.

Heimefrontfjella, a mountain chain 130 km long and up to 30 km wide in western Dronning Maud Land, East Antarctica, is made up of three distinct tectono-metamorphic terranes, namely the Kottas, Sivorg and Vardeklettane terranes. In the north-west lies the Kottas Terrane (Fig. 1), containing rocks typical for amphibolite-facies metamorphic conditions, in the south-west lies the granulite-facies Vardeklettane Terrane, while the central

and eastern parts comprise the large, amphibolite-facies Sivorg Terrane. All three terranes contain mainly rocks of volcano-sedimentary and igneous origin with protolith ages between roughly 1200 and 1100 My that were metamorphosed during the collision of a volcanic arc with the Kaapvaal Craton at approximately 1080 Mya (Jacobs et al. 1996; Bauer, Thomas et al. 2003; Jacobs 2009).

Abbreviations and symbols in this article
 HSZ: Heimefront Shear Zone
 LPO: lattice preferred orientation
 ODF: orientation distribution function
 MPa: mega-pascals
 My: million years
 Mya: million years ago
 X, Y, Z: axes of the finite strain ellipsoid
 (hkl), {hkl}: miller indices of lattice plane and the equivalent form
 <a>, [c]: slip direction parallel to the a and c axes in the hexagonal system
 2 θ : bragg angle
 Ψ , Ω : tilt axis, rotation axis of the goniometer
a: quartz prism {110}
m: quartz prism {100}
r: positive rhombohedron {101} of quartz
z: negative rhombohedron {011} of quartz
 ξ : trigonal bipyramids {112} of quartz

Large parts of the Heimefrontfjella were affected by a second major tectono-metamorphic event at the Ediacaran/Cambrian boundary when East Antarctica collided with the Kalahari Craton during the formation of Gondwana, in the southern part of the huge East African/Antarctic Orogen (Jacobs et al. 2003). The western boundary of this orogen in western Dronning Maud Land is marked by the subvertical HSZ, which separates the Vardeklettane and Kottas terranes from the Sivorg Terrane (Fig. 1). This shear zone originated from the oblique collision between the volcanic arc and the Kaapvaal Craton at around 1080

Mya (Jacobs et al. 1993; Jacobs & Thomas 1994), but it was reactivated during Ediacaran/Cambrian times, as demonstrated by the deformation of certain post-1060 My old dykes (Bauer, Fielitz et al. 2009) and contrasting cooling ages on both sides of this crustal lineament. In the Kottas and Vardeklettane terranes, K–Ar and Ar–Ar mineral cooling ages range from 1010 to 950 My, indicating cooling below 300°C in the early Neoproterozoic. In contrast, the HSZ and all outcrops to the east thereof are characterized by K–Ar and Ar–Ar cooling ages between 570 and 470 My, proving a strong thermal overprint during the Ediacaran/Cambrian tectonic event (Jacobs et al. 1995; Jacobs et al. 1999). These different tectono-metamorphic domains are also reflected by the magnetic anomaly patterns (Golynsky & Jacobs 2001) which shows the continuation of the HSZ under some of the ice-covered areas of Dronning Maud Land.

In the Kottas Terrane the main tectonic elements such as foliations and folds were formed contemporaneously with peak metamorphic conditions, resulting from the late Neoproterozoic arc-continent collision. However, numerous low-angle thrusts, marked by mylonites and ultramylonites were formed during the Ediacaran/Cambrian tectonic event.

Albeit the HSZ and the low-angle thrust zones are known for a long time, no detailed description of their microfabrics nor a conclusive kinematic model has been published. An open question is especially the shear sense of the HSZ. Jacobs et al. (1993) stated that the HSZ formed

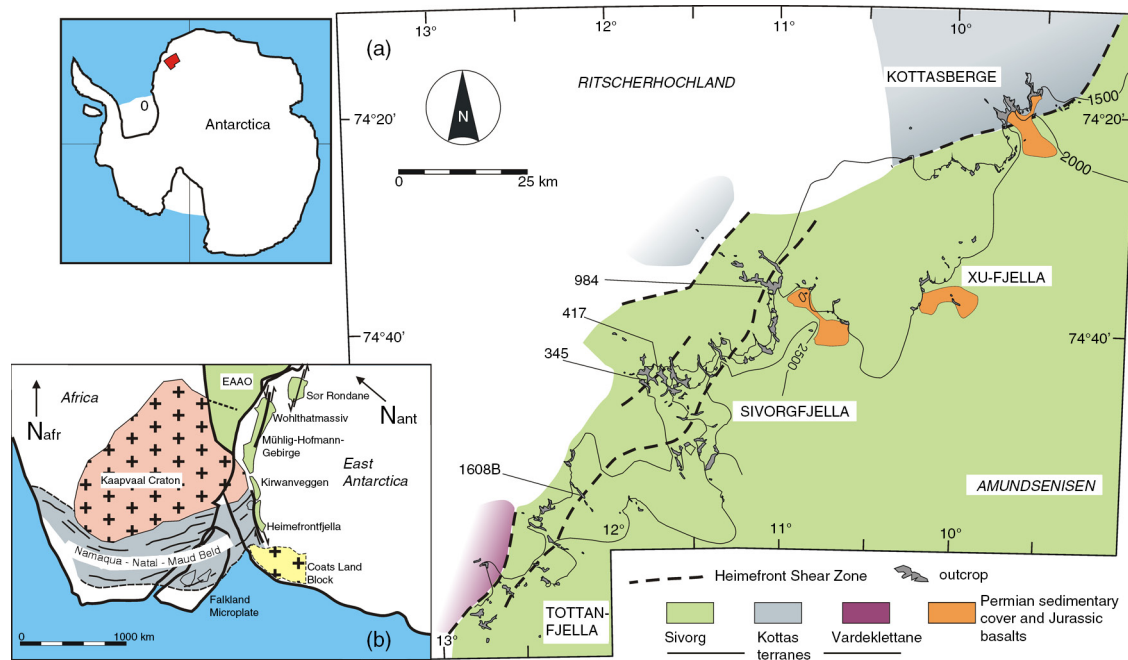


Fig. 1 (a) Geological overview of the Heimefrontfjella and (b) its position in a Gondwana reconstruction (after Jacobs & Thomas 1994).

as a result of indenter tectonics around the southern margin of the Kaapvaal Craton during the collision of the mainly volcanic Maud Belt and its poorly known southern hinterland at about 1080 Mya. Although they showed dextral kinematics, their model would geometrically require an initially sinistral crustal lineament, because in today's African coordinates the continental margin of the Kaapvaal Craton changes from an east–west to a north–south direction immediately north of what is today the Heimefrontfjella.

The objective of this study is to describe the fabric of mylonitic rocks from the Heimefrontfjella and to interpret them in terms of kinematics within the context of the Ediacaran/Cambrian structural evolution of western Dronning Maud Land. For this purpose, we investigate the microfabrics, especially the quartz lattice orientation, from oriented samples representing mylonitic thrusts and protomylonitic high strain zones in the Kottas Terrane. A series of samples have been chosen from the north-western part of the Kottasberge between the northern tip of Brandstorpnabben and the Schivestolen plateau, where a relatively complete section through the Kottasberge is

exposed (Fig. 2). The key question is why such almost horizontal tectonic elements formed in close proximity to the subvertical HSZ and if they were developed together.

Geology of the Kottasberge

The Kottasberge (Milorgfjella in Norwegian) is the northernmost crustal block exposed in the Heimefrontfjella (Fig. 1). The main massif forms the Kottas Terrane, which is mainly composed of juvenile Mesoproterozoic volcanic and plutonic rocks of calc-alkaline composition (Bauer, Jacobs et al. 2003) that were deformed under amphibolite-facies conditions between 1080 and 1060 Mya. Two chains of smaller nunataks in the east and south-west of the main massif show a different lithological and structural composition that resembles those of the southern Sivorg Terrane.

The oldest rock unit of the Kottas Terrane is the Vikenegga Suite (Fig. 2), a banded tonalite–trondhjemite–diorite orthogneiss which has been dated at 1130 ± 17 Mya (Jacobs et al. 1999). A supracrustal sequence, summarized in Fig. 2 as “metavolcanic rocks,” is composed of

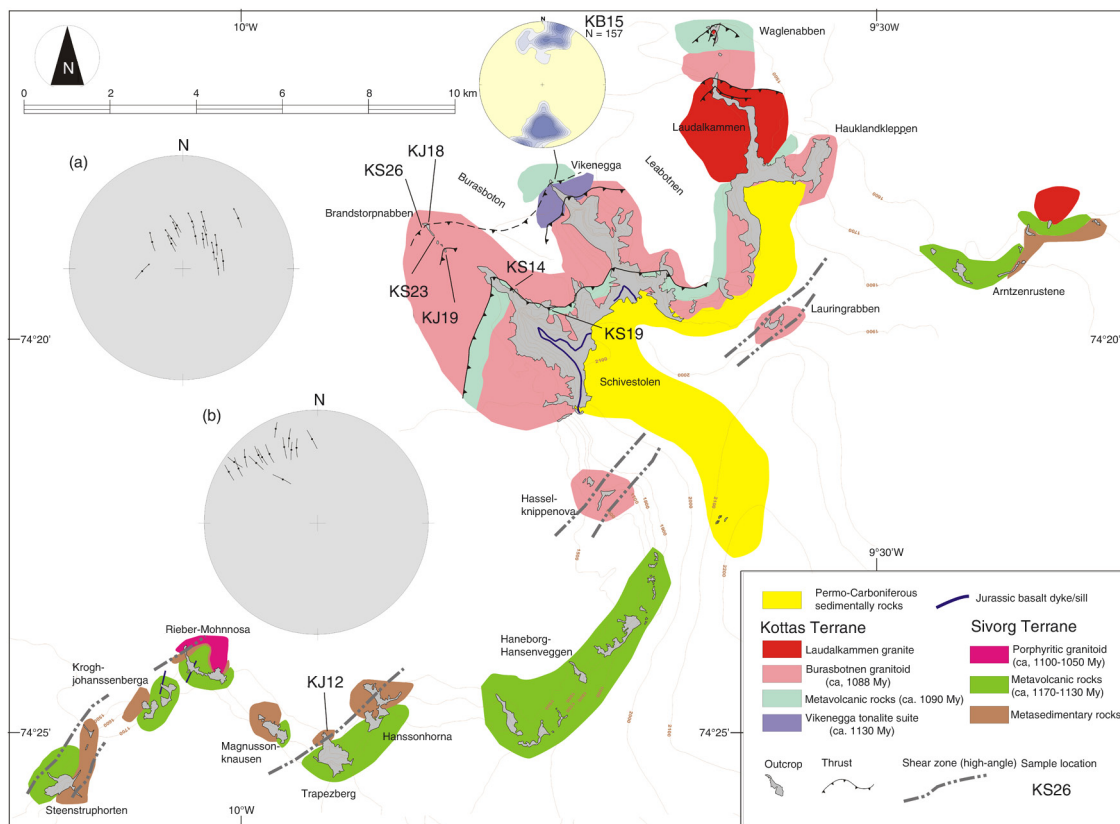


Fig. 2 Geological map of the Kottasberge with sample locations. (a) Stereographic projection of the thrust zones in the Kottas Terrane with the trajectories of the stretching lineations (Hoeppener diagram). (b) Stereographic projection of high-angle shear zones in the south-western nunataks and the trajectories of the stretching lineations. At the top of Vikenegga a quartz c-axis diagram of sample KB15, 157 axes, contours at 1, 2, 3, ... %.



Fig. 3 Examples of shear zones and thrusts in the Kottasberge (a) steep shear zone in bimodal metavolcanic rocks at Trapezberg, sampling site of KJ12, view in north-eastern direction; (b) ductile thrust zone at Brandstornabben, view in south-western direction, the hanging wall moved to the right; (c) ductile thrust zone at Vikenegga, view in south-western direction, the hanging wall moved to the right.

fine-grained, pink felsic gneisses with rhyolitic to rhyodacitic composition and an equigranular fabric. The felsic gneisses are commonly associated with amphibolites and finely banded intermediate gneisses, the latter having been interpreted as metatuffites (Bauer, Jacobs et al. 2009). Zircons from a sample of felsic gneiss gave a conventional U–Pb zircon age of 1093^{+35}_{-39} My (Arndt et al. 1991). The most voluminous rock unit is characterized by coarse-grained, two-feldspar orthogneisses of granitic to granodioritic composition, forming decimetre thick sheets. Conventional U–Pb zircon ages of 1100^{+23}_{-17} My (Jacobs et al. 1999) and 1088 ± 10 My (Arndt et al. 1991) from these gneisses have been interpreted as crystallization ages.

The metamorphic basement is intruded by numerous post-tectonic igneous rocks of granitic and dioritic composition. The most voluminous of these intrusions is exposed at Laudalkammen but the whole Kottas Terrane is “soaked” by pegmatites, aplites and granitic dykes. One of these pegmatites gave a conventional U–Pb zircon age of 1060 ± 8 My (Arndt et al. 1991) which also confines the metamorphism and deformation in the Kottas Terrane to the time span between 1080 and 1060 Mya.

The south-western part of the Kottasberge is a chain of nunataks made up of a sequence of garnet–sillimanite–

biotite paragneisses and bimodal metavolcanic rocks. Another chain of nunataks east of the main mountain massif (Arntzenrustene) is also characterized by meta-sedimentary rocks including calc-silicates and bimodal metavolcanic rocks. These areas are characterized by intense deformation with small-scale schlingen structures and metre-wide subvertical shear zones (Fig. 3a).

Tectonic structures in the eastern part of the Heimefrontfjella as well as in the HSZ itself and the shallow thrusts in the Kottasberge are the result of a major orogeny, associated with amphibolite-facies metamorphism. This event took place between Ediacaran and Ordovician times; the time frame was set by dating the youngest affected igneous dyke (486 ± 7 Mya; Bauer, Fielitz et al. 2003) and the K–Ar cooling age of the $< 2 \mu\text{m}$ fraction in a mylonite from the Kottasberge (473 ± 11 Mya; Jacobs et al. 1995). Metamorphic conditions in the Heimefrontfjella were determined using geothermobarometers, based on exchange reactions between garnet, micas and aluminosilicate assemblages in equilibrium. Schulze (1992) determined 640°C and 1100 MPa as peak metamorphic conditions for the Sivorg Terrane, followed by a retrograde phase at 550°C and 450 MPa. The same methods revealed $580\text{--}480^\circ\text{C}$ and 400–330 MPa for the

southern Kottasberge (Bauer 1995). Mineral assemblages within mylonites do not represent these peak metamorphic conditions, but secondary minerals like chlorite and epidote indicate retrograde conditions in the greenschist-facies for these rocks.

The regional distribution of thrusts is shown in Fig. 2, and their spatial orientation and the orientation of their mineral stretching lineations are summarized in a Hoepfener diagram (Hoepfener 1955) within this figure. Individual thrust zones have a true thickness between 1 and 5 m (Fig. 3b, c) and the boundaries with the adjacent gneisses are generally very sharp. Parallel to these distinct thrust zones are numerous high-strain zones, several metres in thickness, where the transformation from gneiss to protomylonite can be observed.

Analytical methods

A powerful tool for studying the deformation regime and kinematics of mylonites is the analysis of quartz lattice preferred orientation. For a review of the method see Passchier & Trouw (2005, chapter 4.4). Texture development is governed by the active deformation mechanisms, the shape of the finite strain ellipsoid, the strain magnitude and the strain path. Schmid & Casey (1986) demonstrated that the role of these fabric-forming factors can be deduced from measured textures of naturally deformed rocks. Under geological conditions the most effective texture controlling mechanisms are intracrystalline glide (Price 1985) and dynamic recrystallization (e.g., White 1976). Common glide systems in quartz (Nicolas & Poirier 1976; Law et al. 1990) are shown in Table 1.

The effect of dominant slip on easy glide systems in naturally deformed quartz has been discussed by many authors (e.g., Lister & Dornsiepen 1982; Schmid & Casey 1986). The most common types of preferred orientation are: Maximum I (Fig. 4c) with the c-axes parallel to Y arises if prism- $\langle a \rangle$ glide prevails; Maxima II in YZ girdle arise if positive or negative rhomb- $\langle a \rangle$ glide dominates deformation; Maxima III in the XZ plane arise because one of the trigonal bipyramid $\langle c+a \rangle$ systems

dominates deformation; Maximum IV with c-axes parallel to Y arises if mostly the basal- $\langle a \rangle$ glide is active at low deformation temperatures.

The activity of one or more glide systems (in most cases simultaneous) depends on their critical resolved shear stresses, which is affected by deformation temperature, crystal structure, e.g., high/low quartz transition (Kruhl 1996), and the presence of water (Blacic 1975). The influence of other parameters such as strain rate and deformation regime (e.g., pure shear vs. simple shear) has been deduced from experiments and numerical models and compared with naturally deformed quartzites (Tullis et al. 1973; Lister & Hobbs 1980; Schmid & Casey 1986; Stipp et al. 2002). Evidence for non-coaxial deformation is given by asymmetric texture patterns. Quartz c-axis texture patterns produced by different deformation regimes and the position of several submaxima are shown in Fig. 4. The general validity of these results, not only for monomineralic quartzites but also deformed polyphase rocks, has been demonstrated by numerous studies (e.g., Fueten 1992; Stipp et al. 2002; Toy et al. 2008).

The quartz c-axis orientations were measured optically with a conventional U-stage microscope using oriented thin sections. All measurements are displayed in equal area, lower hemisphere projection. The Gaussian method with a kurtosis = 100 was chosen as counting model. The bell-shaped weighting curve has a width at half-height of 8.1° . The resulting contours are equivalent to the conventional counting of 1% fixed circles but with a smoother outline.

For nine samples, quartz textures were also determined using a Siemens x-ray texture goniometer at the Institute for Mineralogy and Economic Geology of the RWTH Aachen, using oriented circular specimens 20 mm in diameter and 5 mm thick. Quartz is the main component of all analysed samples but plagioclase, K-feldspar and biotite are also present, which restricts the application of x-ray texture goniometry. To avoid possible overlap with plagioclase, only pole figures of quartz bipyramids {112} and prism planes {110}, which do not coincide with reflections from plagioclase planes, were measured. Measurement conditions are given in the Supplementary Tables S1 and S2. Pole figures not presented in this study are described by Bauer (1995).

The ODF was calculated from the experimentally measured pole figures with the program Mentex (Schaeber & Siemes 1996). Using this ODF, we recalculated pole figures of the prism **a** {110}, the bipyramid ξ {112}, the prism **m** {100}, the positive rhombohedron **r** {101}, the negative rhombohedron **z** {011} and the basal plane {001}. All pole figures are shown in the XZ plane of the finite

Table 1 Common glide systems in quartz (Nicolas & Poirier 1976; Law et al. 1990).

Plane	hkl indices	Slip direction
Basal	{001}	$\langle a \rangle$
prism m	{100}	$\langle a \rangle$, [c] or [c] + $\langle a \rangle$
prism a	{110}	[c]
rhomboheda r and z	{101} and {011}	$\langle a \rangle$ or [c] + $\langle a \rangle$
rhomboheda $+\pi$ and $-\pi$	{102} and {012}	$\langle a \rangle$ or [c] + $\langle a \rangle$
trigonal bipyramids	{2-12}	[c] + $\langle a \rangle$

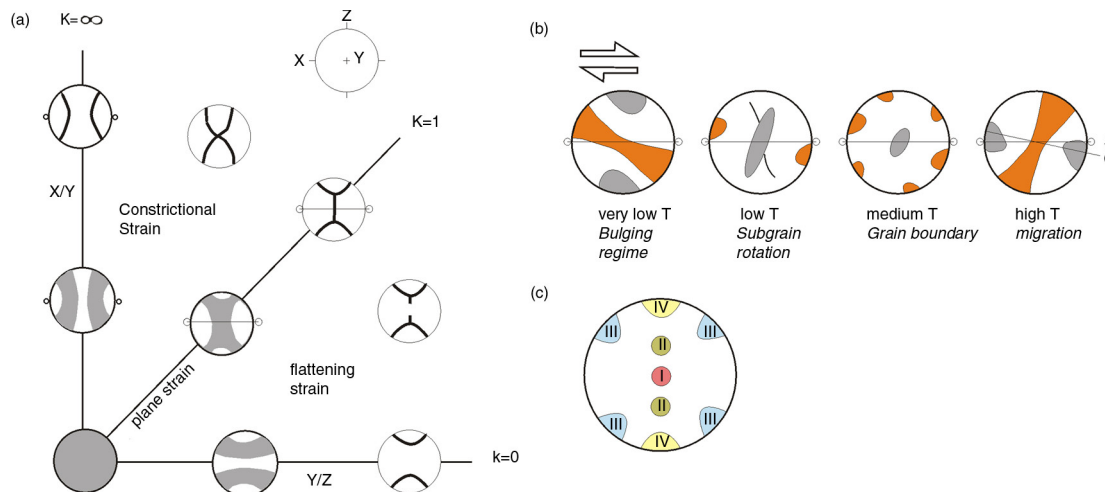


Fig. 4 Pole diagrams showing quartz c-axes/quartz (001) reflection patterns produced by (a) pure shear (Flinn diagram) and (b) simple shear (Schmid & Casey 1986) with the prism **a** poles in orange; (c) positions different types of quartz c-axis maxima, modified from Sander (1950).

strain ellipsoid, where X is defined by the stretching lineation and Z is normal to the mylonitic foliation.

Petrography and microfabrics

Mylonites from the HSZ and the low-angle, ductile thrusts in the Kottasberge display a well-developed foliation and a pronounced stretching lineation. Samples have been optically investigated in the XZ and the YZ sections of the finite strain ellipsoid. Except from the pure quartzite sample 1608B (>98% quartz), all samples contain variable amounts of feldspar and other minor components, including garnet, hornblende and micas. The main mineral, however, is always quartz and samples were carefully selected to avoid specimens with more than 10% mica, which could cause strain partitioning between quartz-rich and quartz-poor domains.

Mylonites of the HSZ

Sample 1608B is an orthomylonitic quartzite from Bowrakammen in the northern Tottanfjella (Fig. 1). The quartzite contains biotite, garnet and plagioclase as minor components with a total amount of accessory minerals of less than 10%. The equilibrium paragenesis of garnet + biotite indicates metamorphism under uppermost greenschist-facies or lowermost amphibolite-facies conditions during the deformation. Some garnet grains have been fragmented and trails of these fragments are aligned parallel to the X-axis of the strain ellipsoid.

Quartz grains form a polygonal mosaic with grain boundaries showing regular 120° triple junctions. Grain sizes are variable, bands of fine quartz below 0.5 mm

diameter alternate with medium-grained quartz with grains up to 3 mm diameter, indicating a type B2 ribbon quartz microfabric (Boullier & Bouchez 1978). The extinction of individual quartz grains is sharp, subgrains are not developed or have been eliminated because of post-tectonic static recrystallization.

Quartz grains of sample 1608B show a strong preferred orientation of all lattice planes (Fig. 5). Individual maxima of the prisms **a** lie in the XZ plane. Poles to the basal plane (001) recalculated from the ODF plot on a YZ girdle with one maximum close to Y and a weaker maximum close to the periphery of the pole figure. This pattern is generally confirmed by the results of optical texture analysis with the U-stage. Here, an additional weak maximum appears with c-axes oriented 10–20° away from Z. These c-axes were measured on small grains that were underestimated by x-ray goniometry owing to their small size. In x-ray texture goniometry grains are measured by their surface, so that larger grains result in higher intensities. In optical measurement each grain is equally weighted. The c-axis texture shows an oblique single girdle, indicating a dextral simple shear component. The pole diagrams in Fig. 5 are oriented with X parallel to the stretching lineation $L = 100/32$ and viewing south. The tectonic transport direction indicated by the asymmetric quartz c-axis fabric is top-to-the-west.

Three additional samples from different parts of the HSZ show similar quartz c-axis patterns. Sample 345 was collected from Bieringmulen in southern Sivorgfjella from the westernmost branch of the HSZ. It is a quartz-rich gneiss with biotite, plagioclase, garnet, epidote and clinzoisite as minor components. Quartz shows an equigranular, polygonal fabric. Neither quartz nor plagioclase

show grain internal deformation features like undulose extinction or deformation lamellae indicating recrystallization under a postkinematic static regime. The quartz c-axis texture (Fig. 5) shows a diffuse type II crossed girdle or very blurred single girdle texture with maxima immediately above and below Y. The texture is symmetric and does not show a shear sense, which is matched by a lack of conclusive shear sense indicators on a macroscopic or microscopic scale although the rock has a pronounced stretching lineation ($L = 055/13$).

Sample 417 (Fig. 5) was taken from a boudinaged paragneiss with garnet, biotite and plagioclase at Norumnuten in central Sivorgfjella. Quartz forms an equigranular polygonal fabric of medium-sized grains. The c-axis pattern is interpreted as a single girdle with a broad maximum near Y and a c-axis-free area near Z. Here again, a clear asymmetry is lacking despite a pronounced stretching lineation ($L = 295/43$).

Sample 984 from Scharffenbergbotnen in northern Sivorgfjella represents the easternmost part of the HSZ.

The rock has been interpreted as a mylonitic felsic meta-volcanic rock with quartz, biotite and plagioclase. The fine-grained dark rock has a smooth mylonitic foliation and a strong mineral stretching lineation ($L = 139/42$). The mostly fine-grained quartz crystals show slightly interlobate grain boundaries, undulose extinction and are elongated. The long axis of the grains has an angle of 25° with the mylonitic S plane, forming an oblique foliation *sensu* Berthé et al. (1979). The c-axis pattern (Fig. 5) shows a single oblique girdle with a broad maximum at Y and weaker submaxima on the YZ girdle and close to Z, indicating a sinistral sense of shear in the sample reference frame. Here at the eastern margin of the HSZ, the mylonitic foliation is dipping with 53° to the southwest (250° dip direction). With a normal, top-to-the-south-east movement, this sample probably represents oblique Riedel shears at an angle of approximately 45° to the overall strike in that segment of the HSZ.

Sample KJ12 was collected from the northern part of the HSZ in the south-western nunataks of the Kottas-

Sample	1608B	345	417	984	KJ12
Prism a		not measured	not measured	not measured	
Base (001)		not measured	not measured	not measured	
c					
Comments	s 144/45 L 100/32 annealed 300 axes	s 130/87 L 055/13 annealed 300 axes	s 250/53 L 295/45 annealed 200 axes	s 124/45 L 139/42 annealed 300 axes	s 140/41 L 111/35 partially annealed 250 axes

Fig. 5 Pole diagrams and quartz c-axis diagrams of mylonites from the HSZ. Quartz LPOs (x-ray texture goniometry) of prism a, recalculated from measured pole figures. Base (001) calculated from ODF. Contours at 1.0, 1.2, 1.4 . . . times uniform distribution. Quartz c-axis presented in an equal area projection, lower hemisphere, contours 1, 2, 3 . . . %. All diagrams are shown in the XZ cut of the finite strain ellipsoid with Z at the top and X in horizontal direction.

berge in a transitional position between the steep HSZ and the low-angle ductile thrusts. The foliation is dipping at a moderate angle towards the south-east with a pronounced stretching lineation plunging east–south-east. The rock is a two-mica paragneiss with minor amounts of garnet and thin quartz layers that were locally folded. The quartz is fine-grained, showing dynamically recrystallized grains that are slightly elongated in the *s* plane of the strain ellipsoid whereas the biotite crystals form a type II S-C fabric (Lister & Snoke 1984). Pole figures for (001) and the *c*-axes (Fig. 5) are characterized by a single girdle from Z over Y with a maximum at Y. Poles of both, the **a** prisms, plot in the XZ plane of the strain ellipsoid with maxima close to X. The girdle texture is not oblique but the S-C fabric indicates a dextral, west–north-west directed simple shear component.

Mylonites of the thrust zones in the Kottas Terrane

Sample KS23 is a protomylonitic augen gneiss from the northern tip of Brandstornabben. This sample represents a quartz-rich variety of the coarse grained biotite-two-feldspar gneiss that forms large parts of the Kottas Terrane. The rock has been collected from the margin of a ductile thrust, ca. 4 m thick, outside of the orthomylonitic zone. Feldspars are generally fragmented and the cores of plagioclases are saussuritized, indicating low-temperature alteration. Quartz is present in two grain types: highly deformed, large porphyroclasts with undulose extinction that are elongated parallel to the X direction and fine recrystallized grains with polygonal to weakly interlobate crystals and a grain size of $33.3 \pm 15.3 \mu\text{m}$.

The pole diagram for (001) (Fig. 6) shows a pattern with rudimentary small circles around Z with an opening angle of approximately 90° . The connecting girdle over Y is weakly developed with a gap at Y. This pattern is confirmed by the results of optical texture analysis with the U-stage. Individual maxima of the prism **a** lie on two great circles around Z, which almost meet at Y. The (001) and the corresponding **a** pole figures are typical for flattening strain where $\langle a \rangle$ axes cluster in circles around the shortening direction (Schmid & Casey 1986). The texture results from a deformation under mainly pure shear conditions with a weak simple shear component that is responsible for the asymmetry in the pattern. The simple shear component becomes visible in the optical analysis of the deformed, elongated quartz porphyroclasts. They have been plotted in a separate diagram (Fig. 6), showing a strongly oblique single girdle texture. The simple shear direction deduced from these porphyroclasts is top-to-the-north–north-west.

The leucocratic augen gneiss KJ19 is from a ductile thrust zone in the southernmost nunatak of the Brandstornabben group. The rock is a quartz-rich gneiss of broadly granitic composition with mesoperthite, microcline and plagioclase as well as minor biotite. The feldspars show signs of an earlier ductile deformation with flame-shaped deformation lamellae and subgrain formation. During a later stage these have been fragmented. Quartz crystals form fine-grained aggregates with a polygonal, equigranular fabric. This fabric, which was formed by static recrystallization, was also overprinted by a later deformation that formed submillimetric shear planes with very fine-grained dynamically recrystallized quartz grains.

This two-phase deformation phase is reflected in the quartz LPO (Fig. 6). With the U-stage 200 grains of the isometric, polygonal quartz grains have been measured. The grain size distribution is uniform with $0.05 \pm 0.01 \text{ mm}$. In contrast, within the late shear planes the grain size was reduced below $5 \mu\text{m}$ which does not allow an optical determination of the *c*-axes. The quartz *c*-axes are arranged in a type II crossed girdle fabric with a main maximum at Y. This is a typical pattern of prism– $\langle a \rangle$ glide. In the pole figure of the base (001) this crossed girdle is not recognizable since the influence of the very fine grains in the shear planes is also recorded. The pole figure of the **a** prism shows distinct maxima close to X. Such patterns are explained by a low temperature overprint of an originally medium temperature texture. Figure 4b shows the development of quartz textures under different temperature conditions. The *c*-axes show a strong maximum at Y which would require three separate **a** maxima in the XZ plane. In the discrete, fine-grained shear planes this pattern is overlain by an oblique girdle with a single maximum of the prism **a** plane. However, this single girdle seems to be somewhat de-centred from Y indicating a different orientation of the strain ellipsoid between early and late deformation. Asymmetric trails of fragmented feldspars indicate a top-to-north-west transport during the final deformation phase.

KS26 is an orthomylonite from the Brandstornabben nunatak group, taken from the main thrust zone. The composition is broadly granitic with some low temperature alteration. Most of the biotite was retrogressed to chlorite. Quartz crystals show a grain size distribution between 0.05 and 0.5 mm with interlobate grain boundaries. Elongate quartz grains and biotite/chlorite flakes form a S-C fabric. Most of the prism **a** poles (Fig. 6) plot in the centre of the XZ plane of the strain ellipsoid. The *c*-axes and (001) poles are arranged on a single girdle between Z and Y which is somewhat inclined

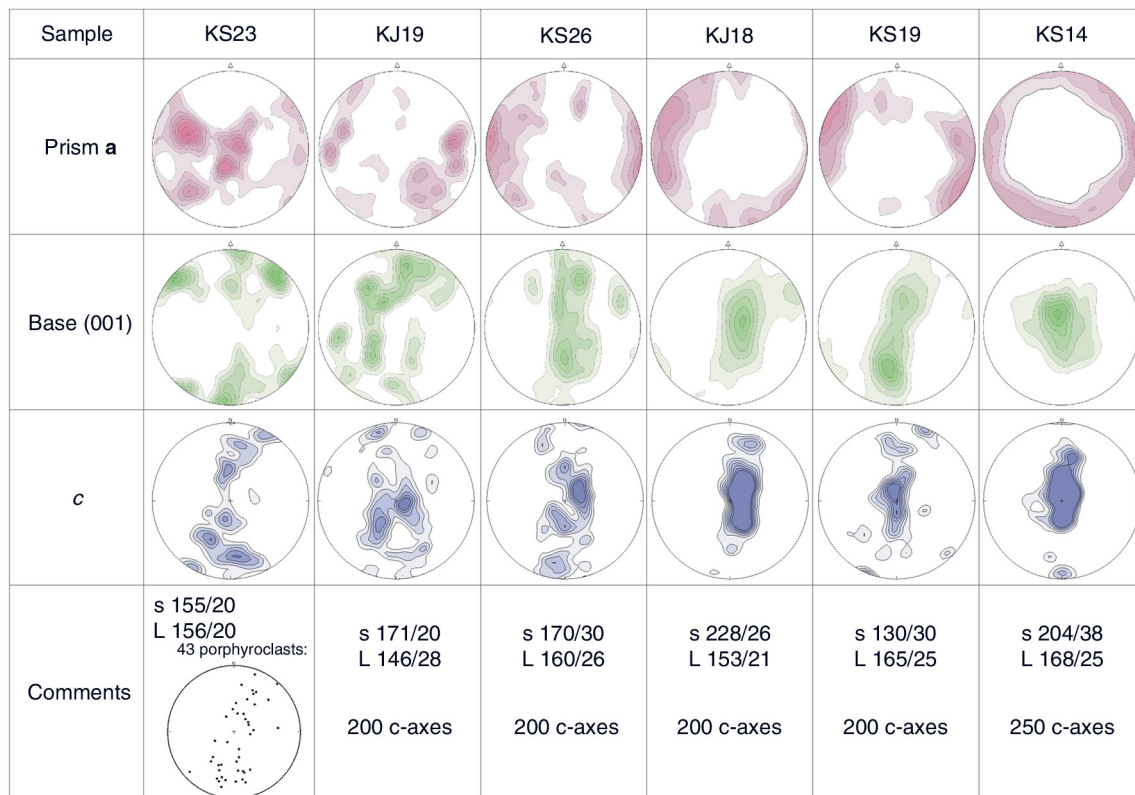


Fig. 6 Pole diagrams and quartz c-axis diagrams of mylonites from ductile thrusts in the Kottasberge. Quartz LPOs (x-ray texture goniometry) of prism **a**, recalculated from measured pole figures. Base (001) calculated from ODF. Contours at 1.0, 1.2, 1.4 ... times uniform distribution. Quartz c-axis presented in an equal area projection, lower hemisphere, contours 1, 2, 3 ... %. All diagrams are shown in the XZ cut of the finite strain ellipsoid with Z at the top and X in horizontal direction.

in a clockwise sense. This sense of shear indicates a top-to-the-north-west tectonic transport.

A second sample from the core of this 4 m thick thrust zone is the ultramylonite KJ18. The rock has a similar granitic composition like KS26 but it is a fine-grained rock with less than 10% preserved porphyroclasts. The remaining plagioclase porphyroclasts show deformation twinning, often kinked, and internal microfractures with very small recrystallized grains along those fractures. Common are also asymmetric feldspar σ -porphyroclasts with recrystallized plagioclase and quartz in the pressure shadows. Quartz occurs throughout the matrix but also concentrated in up to 0.4 mm thick quartz ribbons (type B2b after Boullier & Bouchez 1978) with internal grain sizes ranging from 0.01 to 0.1 mm. The quartz grains are slightly elongated with long axes at an angle of approximately 25° to the ribbon boundaries. The quartz in the matrix has significantly finer grain sizes of $20.8 \pm 6.5 \mu\text{m}$.

The c-axes show a high degree of preferred orientation with a peak near Y of 11.5% per 1% of the Schmidt Net (Fig. 6). In contrast the (001) pole diagram shows a much weaker degree of preferred orientation which reflects the

high amount of very small grains that are underrepresented in the c-axes measurement. Such grains often react to flow stress with grain boundary sliding which has a negative effect on the preferred orientation (see discussion by Passchier & Trouw 2005). However, both the (001) and c-axes pattern are similar, showing a YZ girdle. The prism **a** poles are arranged in two maxima close to X in the XZ plane within a short distance of 30° . The sense of shear in the ultramylonite indicated by numerous σ -clasts is top-to-the-north-west.

Sample KS19 was taken from the southernmost thrust zone in the Kottas Terrane that can be traced throughout most of the main massif (Fig. 3). The rock has a fine-grained, felsic composition with quartz, plagioclase, muscovite, biotite and clinozoisite, a retrogression product of garnet which is preserved in relics only. Plagioclase porphyroclasts show undulose extinction and deformation lamellae. Quartz crystals show subgrain boundaries and weakly interlobate grain boundaries. Type B2a quartz ribbons are common with smooth internal quartz–quartz boundaries. The texture of the c-axes and the (001) poles

shows a single girdle from Z over Y with maxima approximately 25° away from Y (Fig. 6). The prism **a** poles are arranged in a broad maximum near X with the weak relic of a joining great circle. The sense of shear is top-to-the-north–north-west.

KS14 is a sample from the same thrust zone in the main massif of the Kottasberge but it was taken from further north than KS19. The rock has a slightly different composition, since the ductile thrust is cutting through a band of felsic metavolcanic rocks with K-feldspar and little mica. Both feldspars form fragments of up to 0.5 mm diameter. Mica and secondary epidote is concentrated on the mylonitic *s* planes. Quartz crystals form core-and-mantle structures (White 1976) with porphyroclasts rich in subgrains, surrounded by fine-grained, dynamically recrystallized grains with weak undulose extinction and an average grain size of $26.9 \pm 10.2 \mu\text{m}$.

The *c*-axes and the (001) are arranged on a broad maximum at Y (Fig. 6). This maximum is stretched on both sides towards Z. Single maxima at Y have been interpreted as a result of medium temperature deformation under simple shear conditions; however, such textures show generally three distinct **a** maxima in the XZ plane with a distance at 120° to each other (see Fig. 4b and Passchier & Trouw 2005). In our case the **a** prism poles are arranged almost symmetrically in the XZ plane without distinctive maxima. Such unusual textures were described by Mancktelow (1987) from the greenschist-facies Simplon Fault Zone in the Alps. The *c*-axes/(001) pole maximum is a result of prism- $\langle a \rangle$ glide but at high-strain rates subgrains form by lattice kinking and bending around a rotation axis which is parallel to the *c*-axis of the host grains, i.e., the *c*-axes remain centred at Y but the prism **a** poles will not form distinctive maxima.

Discussion

A common feature of the mylonites from the HSZ is the presence of strain-free grains with polygonal quartz domains, showing grain boundaries with typical 120° triple junctions (Fig. 7a). These signs of static recrystallization (annealing) has, according to experimental studies by Heilbronner & Tullis (2002) no significant effect on the overall pattern of the quartz LPO/*c*-axis orientation, except that the strength could decrease. The measured textures (Fig. 5) show such signs, there maxima are quite broad and are, especially for the **a** prisms quite blurred. Samples 417, 984 and KJ12 show single girdle patterns with the main peak at Y. This pattern results from a combination of prism- $\langle a \rangle$ glide (maximum at Y) and intracrystalline gliding on the positive (**r**) and negative (**z**) rhombs (Lister & Dornsiepen 1982) producing maxi-

ma close to Y on the YZ branch of a single girdle. These intracrystalline slip systems are generally observed in metamorphic rocks of at least upper greenschist-facies (e.g., Fueten et al. 1991; Stipp et al. 2002).

In samples 1608B and 984 the maximum at Y is less pronounced, the single girdle texture is better developed. The pattern is typical for prism- $\langle a \rangle$ glide with a minor basal+rhomb- $\langle a \rangle$ glide that was produced the sub-maximum close to Z (Jessel 1988). In naturally occurring mylonites and experimental studies, such complete girdle textures are associated with lower temperatures than textures with a single point maxima near Y (Stipp et al. 2002; Pennacchioni et al. 2010).

More informative are the non-annealed rocks from the thrust zones in the Kottas Terrane which preserve their mylonitic microstructures. Based on experimental studies by Hirth & Tullis (1992), and confirmed in naturally occurring mylonites with good temperature control (Stipp et al. 2002), characteristic microstructures of recrystallized quartz can be subdivided in three dislocation creep regimes. Bulging recrystallization starts along quartz grain boundaries and, to a minor extent, along microcracks in porphyroclasts at temperatures of $280^\circ \pm 30^\circ\text{C}$. At such low temperatures (lower greenschist-facies), intracrystalline slip produces quartz *c*-axis/(001) point maxima close to or small circles around Z. Schmid & Casey (1986) interpreted these patterns as a result of dominant basal $\langle a \rangle$ -slip with some contribution of rhomb $\langle a \rangle$ -slip. In samples from the northern tip of Vikenegga and Brandstorpnbaben, such low-grade or greenschist-facies metamorphic conditions are proven by the presence of minerals parageneses with sericite, chlorite and epidote \pm clinozoisite. The quartz grains in these mylonites show undulose extinction, deformation lamellae and numerous, very small subgrains along porphyroclast boundaries and internal fractures, typical for the bulging recrystallization regime (Hirth & Tullis 1992). A resulting quartz *c*-axis texture with a broad maxima near Z is shown in Fig. 2.

At temperatures between roughly 400° and 500°C subgrain rotation recrystallization prevails, resulting in typical core and mantle microstructures. Such microstructures are common in the mylonitic rocks of the Kottas Terrane (Fig. 7b–d).

At such temperatures typical for upper greenschist-facies conditions (and therefore probably at an earlier stage of the tectonic exhumation), basal- $\langle a \rangle$ and prism- $\langle a \rangle$ glide are active, leading to very elongate quartz porphyroclasts with internal subgrain boundaries, almost parallel to the mylonitic shear plane (Fig. 7b). Grains are mainly elongated in the X direction of the finite strain ellipsoid. Such highly strained old quartz

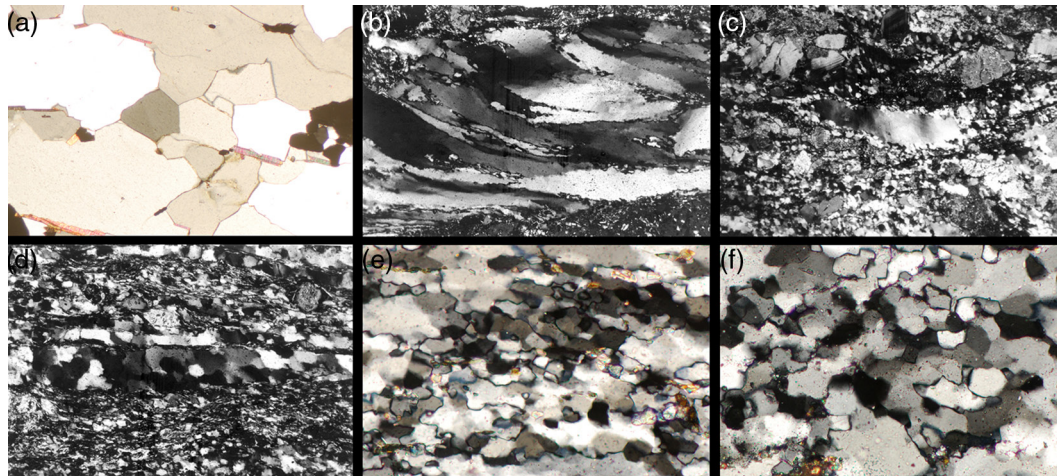


Fig. 7 Microphotographs in the XZ plane of the finite strain ellipsoid, crossed polars: (a) orthoquartzite 1608B from the HSZ, grains annealed (width of the field of view 1.84 mm); (b) protomylonitic augen gneiss from Leabotnen showing elongated quartz crystals with numerous subgrain boundaries and beginning recrystallization along the grain margins (width of field of view 1.3 mm, polarizer and analyser both rotated by ca. 45°); (c) protomylonitic augen gneiss KS23, Brandstornabben, quartz with core and mantle structure (width of field of view 3.2 mm); (d) orthomylonite KS19 from Buråsbotnen with ribbon quartz (width of field of view 1.3 mm); (e) ultramylonite KJ18, centre of the Brandstornabben thrust, polygonal recrystallized grains with few larger porphyroclasts (width of field of view 0.46 mm); (f) ultramylonite KS14, centre of the Buråsbotnen thrust, polygonal pattern of recrystallized grains (width of field of view 0.46 mm).

grains pass laterally into domains of small, dynamically recrystallized new grains. The new grains grow as a result of subgrain rotation in combination with grain boundary migration. The latter can be identified by local bulges of porphyroclasts, which have still the same c-axis orientation than the parental porphyroclasts. Samples with such so-called quartz core and mantle structures such as KS23 (Fig. 7c) and KJ19 are characterized by (rudimentary) type I crossed girdle textures in transition to an oblique single girdle texture (Lister 1981). The patterns combine small circles around Z and a girdle across Y which can be oblique when the rock underwent a deformation with a major rotational (simple shear) component. This crossed girdle pattern is a result of prism- $\langle a \rangle$ glide and contemporaneously gliding on the positive r and negative z rhombs (Schmid & Casey 1986).

With increasing temperatures or higher shear stress/strain rates, domains of recrystallized quartz grains are composed of individual grains that are elongated with the long axis forming an angle between 30° and 50° with the trail of the mylonitic s plane. Such grains are strongly oriented and display oblique girdle textures (e.g., KJ18, Figs. 6 and 7e). The main recrystallization process is still subgrain rotation.

Quartz ribbons are a common feature in mylonitic rocks from the Kottas Terrane. They may have formed during a crack-seal process at high strain rates (Mackinnon et al. 1997) especially when they show an echelon alignment. Such textures are common in the orthomylonites KJ18

and KS19 which show type B2 ribbon quartz (Fig. 7d) according to the classification of Boullier & Bouchez (1978), with internal polygonal quartz aggregates and smooth ribbon boundaries. Individual grains inside the ribbons are slightly elongate with angles around 45° with respect to the outer ribbon boundaries. These mylonites with ribbon quartz and fine-grained equigranular quartz domains with elongated recrystallized grains show very similar c-axis oblique girdle textures. The main maxima are generally developed close to Y, indicating prism- $\langle a \rangle$ as the main glide process (Culshaw & Fyson 1984). KS19 shows a textbook example of an oblique single girdle, resulting from dominant simple shear deformation at medium temperatures where prism- $\langle a \rangle$, basal $\langle a \rangle$ as well as gliding on the positive and negative rhombs is active (e.g., Schmid & Casey 1986; Passchier & Trouw 2005).

At temperatures exceeding 500°C, irregular cusped-lobate to amoeboid quartz grain boundaries develop. Such structures are absent in samples from the Heimefrontfjella. This temperature would produce textures with a point maximum at X which has also not been recorded. Therefore, we assume that all investigated shear zones were active within the subgrain rotation regime (Hirth & Tullis 1992) between 400° and 500°C. This is supported by petrographical evidence. Experimental and empirical data (e.g., Pryer 1993) indicate that the dynamic recrystallization of plagioclase starts at temperatures between 450 and 500°C. In the mylonites

of the Kottasberge plagioclase generally shows stress-induced twinning lamellae which start at the grain boundary and end within the grain. Larger grains of mylonites that have been developed in rocks of granitic origin are often fragmented with very small rims or trails of recrystallized plagioclase along microshear zones. These textures are common in rocks with beginning ductile behaviour of feldspar and therefore the temperature range 450°–500°C is assumed to mark the onset of the tectonic exhumation. The low-temperature mylonite from the northern tip of Vikenegga (Fig. 2 inset), which shows only intracrystalline glide (c-axis maxima at Z) and a greenschist-facies paragenesis, represents probably the youngest thrust during the final stage of the tectonic exhumation. The exhumation of the Kottas Terrane, where low-angle thrust onto a stable, cool Late Mesoproterozoic foreland led to rapid cooling, preserved the microstructures in the mylonites. In contrast, within the HSZ horizontal shortening led to a crustal thickening, indicated by schlingen tectonics with steep fold axes. This hot crust was not rapidly exhumed which led to a post-tectonic static recrystallization in the hot crusts. It can almost be excluded that this annealing was triggered by magmatism, as neither in the exposures nor in the available aerogeophysical data for the ice-covered area have igneous bodies been identified.

For the overall texture development in the mylonites of the Kottas Terrane, we can therefore assume a temperature drop of roughly 150° between peak (realised in the orthomylonite KJ12 of Trapezberg and the mylonites of the HSZ) and terminal metamorphic conditions (realised in the basal- <a> quartz textures of KB15 at northern Vikenegga) which would correspond to a vertical exhumation of 5 km at normal thermal gradients in the crust. However, considering that in the foreland of an active collision orogen generally elevated geothermal gradients prevail, the amount of vertical exhumation could be significantly lower than 5 km.

Conclusions

The prevailing quartz LPO and c-axis textures in mylonites from the Heimefrontfjella show mostly single girdle patterns, some of them with a strong maximum near the Y axis of the finite strain ellipsoid. Such patterns are the result of deformation within the subgrain rotation regime (Hirth & Tullis 1992) close to upper temperature limit of 500°C. The HSZ was formed within or at the western margin of a thickened orogen and were not rapidly exhumed due to the prevailing strike-slip movement within the shear zone. Therefore mylonites from the HSZ show post-tectonic annealing, indicating slow cooling.

The mylonites from the Kottas Terrane still preserve their original microstructures, typical for dynamic recrystallization because of their thrusting onto a cool foreland, which rapidly cooled below the threshold temperature of 280°C.

In order to draw a conclusive model for the tectonic evolution of the Kottas Terrane and its surrounding area, we have to consider following field observations and laboratory results: (1) at least four major, low-angle thrusts >1 m thick and numerous smaller ductile shear zones cut through the Mesoproterozoic basement of the Kottas Terrane; (2) shear sense indicators such as asymmetric clasts, mica fish and S-C fabrics as well as quartz-c-axis textures indicate north–north-west directed tectonic transport on these thrusts and shear zones under simple shear conditions; (3) the presence of chlorite replacing garnet and epidote, zoisite and sericite replacing plagioclase indicate retrograde, greenschist-facies conditions during the tectonic transport, whereas the host rocks still preserve their amphibolite-facies assemblages; (4) Ediacaran/Cambrian-aged low-angle thrusts are absent in other parts of the Heimefrontfjella, alpine-type nappe tectonics in the other terranes have never been recorded; (5) the subvertical HSZ shows an arcuate outline with a change in strike from south-west–north-east to north–south trend along the eastern margin of the Kottas Terrane (Fig. 1); (6) rocks of the HSZ that lack or show only very weak asymmetrical quartz textures are typical for pure shear conditions which is in accordance with the distinct stretching lineations and without clear shear sense indicators.

To accommodate these observations, we suggest that the HSZ developed under a transpressive, weakly dextral tectonic regime. North-west of the anticlockwise bend in the HSZ and about 3–4 km from its western margin a set of north–north-west directed thrusts form a positive flower structure (Fig. 8). In contrast, on the eastern side of the HSZ, for example at Arntzenrustene, gently south-east plunging, open folds prevail. The HSZ was active as a transpressive shear zone in Ediacaran/Cambrian times when the East Antarctic Craton collided with the Kalahari Craton in southern Africa. Kinematics and rheology of a transpressive shear zone in relation to plate motion and strain have been discussed by Tikoff & Teyssier (1994). Once activated, a transpressive, subvertical shear zone predominantly accommodates the strike-slip component during an oblique plate collision. To accommodate the simple shear component, strain partitioning is leading to the formation of low-angle thrusts with a strike parallel to the subvertical shear zone (Tikoff & Teyssier 1994). In the Heimefrontfjella, these thrusts are exposed in the northern part, where they form meter

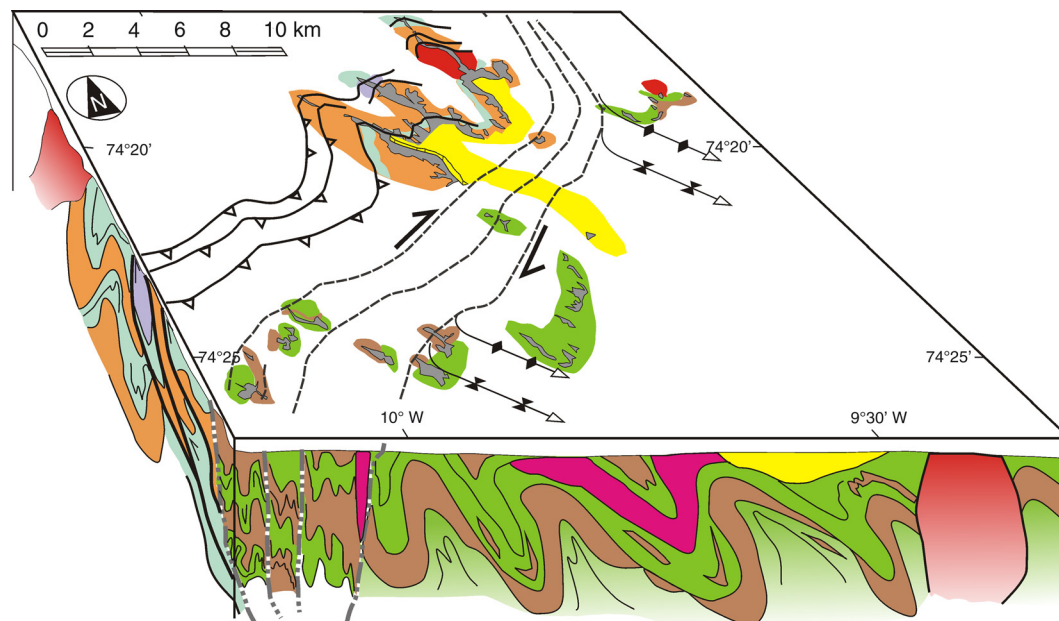


Fig. 8 Block diagram showing the Kottas Terrane as the north-west foreland of the transpressive HSZ. The arrow indicates the current Antarctic north.

thick mylonitic shear zones. For a full analysis of the kinematics of the HSZ it would be necessary to study the eastern margin of the orogeny. The plate which collided with the Kalahari Craton is, however, completely covered by the ice of East Antarctica and the central part of the East African/Antarctic Orogen contains cratonic blocks which are poorly studied and with an unknown plate motion (Jacobs et al. 2015).

Acknowledgements

Funding for this study provided by the German Science Foundation within the project Gesteinsbestand und strukturelle Entwicklung der Heimefrontfjella/Antarktika (Sp 235/8) is gratefully acknowledged. The fieldwork was logistically supported by the Alfred Wegener Institute. This manuscript has greatly benefited from the reviews by L.F.G. Morales, H. Stünitz, S. Oriolo and R.J. Thomas. We also would like to thank H. Goldman for the editorial handling. This is a contribution to the IGCP 648 Supercontinent Cycles and Global Geodynamics project.

References

- Arndt N.T., Todt W., Chauvel C., Tapfer M. & Weber K. 1991. U–Pb zircon age and Nd isotopic composition of granitoids, charnockites and supracrustal rocks from Heimefrontfjella, Antarctica. *Geologische Rundschau* 80, 759–777.
- Bauer W. 1995. *Strukturentwicklung und Petrogenese des Grundgebirges der nördlichen Heimefrontfjella (westliches Dronning Maud Land/Antarktika)*. (Structural evolution and petrogenesis of the metamorphic basement complex of the northern Heimefrontfjella [western Dronning Maud Land/Antarctica].) *Berichte zur Polarforschung* 171. Bremerhaven: Alfred Wegener Institute.
- Bauer W., Fielitz W., Fanning C.M., Jacobs J. & Spaeth G. 2003. Mafic dykes from Heimefrontfjella and implications for the post-Grenvillian to pre-Pan-African geological evolution of western Dronning Maud Land (Antarctica). *Antarctic Science* 15, 379–391.
- Bauer W., Fielitz W., Jacobs J. & Spaeth G. 2009. Neoproterozoic mafic dykes of the Heimefrontfjella (East Antarctica). *Polarforschung* 79, 33–38.
- Bauer W., Jacobs J., Fanning C.M. & Schmidt R. 2003. Late Mesoproterozoic arc and back-arc volcanism in the Heimefrontfjella (East Antarctica) and implications for the palaeogeography at the southeastern margin of the Kaapvaal-Grünhogna Craton. *Gondwana Research* 6, 449–465.
- Bauer W., Jacobs J., Thomas R.J., Spaeth G. & Weber K. 2009. Geology of the Kottas Terrane, Heimefrontfjella (East Antarctica). *Polarforschung* 79, 23–28.
- Bauer W., Thomas R.J. & Jacobs J. 2003. Proterozoic–Cambrian history of Dronning Maud Land in the context of Gondwana assembly. In M. Yoshida et al. (eds.): *Proterozoic East Gondwana: supercontinent assembly and breakup*. Pp. 247–269. London: Geological Society of London.
- Berthé D., Choukroune P. & Jegouzo P. 1979. Orthogneiss, mylonite and non-coaxial deformation of granites: the example of the South Armoricain Shear Zone. *Journal of Structural Geology* 1, 31–42.
- Blacic J.D. 1975. Plastic deformation mechanisms in quartz: the effect of water. *Tectonophysics* 27, 271–294.

- Boullier A.M. & Bouchez J.L. 1978. Le quartz en rubans dans les mylonites. (Ribbon quartz in mylonites.). *Bulletin Soci  t   g  ologique France* 20, 253–262.
- Culshaw N.G. & Fyson W.K. 1984. Quartz ribbon in high grade granite gneiss: modifications of dynamically formed quartz c-axis preferred orientation by oriented grain growth. *Journal of Structural Geology* 6, 663–668.
- Fueten F. 1992. Tectonic interpretations of systematic variations in quartz c-axis fabrics across the Thompson Belt. *Journal of Structural Geology* 14, 775–789.
- Fueten F., Robin P.Y.F. & Stephens R. 1991. A model for the development of a domainal quartz c-axis fabric in coarse-grained gneiss. *Journal of Structural Geology* 13, 1111–1124.
- Golynsky A. & Jacobs J. 2001. Grenville-age versus Pan-African magnetic anomaly imprints in western Dronning Maud Land, East Antarctica. *Journal of Geology* 109, 136–142.
- Heilbronner R. & Tullis J. 2002. The effect of static annealing on microstructures and crystallographic preferred orientations of quartzites experimentally deformed in axial compression and shear. In S. de Meer et al. (eds.): *Deformation mechanisms, rheology and tectonics: current status and future perspectives*. Pp. 191–218. London: Geological Society of London.
- Hirth G. & Tullis J. 1992. Dislocation creep regimes in quartz aggregates. *Journal of Structural Geology* 14, 145–159.
- Hoepfener R. 1955. Tektonik im Schiefergebirge. (Tectonics of the Rhenish Schiefergebirge.). *Geologische Rundschau* 44, 25–58.
- Jacobs J. 2009. A review of two decades (1986–2008) of geochronological work in Heimefrontfjella, and geotectonic interpretation of western Dronning Maud Land, East Antarctica. *Polarforschung* 79, 47–57.
- Jacobs J., Ahrendt H., Kreutzer H. & Weber K. 1995. K–Ar, ⁴⁰Ar–³⁹Ar and apatite fission track evidence for Neoproterozoic and Mesozoic basement rejuvenation events in the Heimefrontfjella and Mannefallknausane. *Precambrian Research* 75, 251–262.
- Jacobs J., Bauer W., Spaeth G., Thomas R.J. & Weber K. 1996. Lithology and structure of the Grenville-age (~1.1 Ga) basement of Heimefrontfjella (East Antarctica). *Geologische Rundschau* 85, 800–821.
- Jacobs J., Elburg M., L  ufer A., Kleinhanns I.C., Henjes-Kunst F., Ruppel A.S., Damaske D., Montero P. & Bea F. 2015. Two distinct Late Mesoproterozoic/Early Neoproterozoic basement provinces in central/eastern Dronning Maud Land, East Antarctica: the missing link, 15–21 E. *Precambrian Research* 265, 249–272.
- Jacobs J., Fanning C.M. & Bauer W. 2003. Timing of Grenville-age vs. Pan-African medium- to high grade metamorphism in western Dronning Maud Land (East Antarctica) and significance for correlations in Rodinia and Gondwana. *Precambrian Research* 125, 1–20.
- Jacobs J., Hansen B.T., Henjes-Kunst F., Thomas R.J., Bauer W., Weber K., Armstrong R.A. & Cornell D.H. 1999. New age constraints on the Proterozoic/Lower Palaeozoic evolution of Heimefrontfjella, East Antarctica, and its bearing on Rodinia/Gondwana correlations. *Terra Antarctica* 6, 377–389.
- Jacobs J. & Thomas R.J. 1994. Oblique collision at 1.1 Ga along the southern margin of the Kaapvaal continent, SE Africa. *Geologische Rundschau* 83, 322–333.
- Jacobs J., Thomas R.J. & Weber K. 1993. Accretion and indentation tectonics at the southern edge of the Kaapvaal craton during the Kibaran (Grenville) orogeny. *Geology* 21, 203–206.
- Jessel M.W. 1988. Simulation of fabric development in recrystallizing aggregates. I. Description of the model. *Journal of Structural Geology* 10, 771–778.
- Kruhl J. 1996. Prism- and basal-parallel subgrain boundaries in quartz: a microstructural geothermobarometer. *Journal of Metamorphic Geology* 14, 581–589.
- Law R.D., Schmid S.M. & Wheeler J. 1990. Simple shear deformation and quartz crystallographic fabrics: a possible natural example from the Torridon area of NW Scotland. *Journal of Structural Geology* 12, 29–45.
- Lister G.S. 1981. The effect of basal-prism mechanism switch on fabric development during plastic deformation of quartzite. *Journal of Structural Geology* 3, 67–75.
- Lister G.S. & Dornsiepen U.F. 1982. Fabric transitions in the Saxony granulite terrain. *Journal of Structural Geology* 4, 81–92.
- Lister G.S. & Hobbs B.E. 1980. The simulation of fabric development during plastic deformation and its application to quartzite: the influence of deformation history. *Journal of Structural Geology* 2, 355–370.
- Lister G.S. & Snoke A.W. 1984. S-C mylonites. *Journal of Structural Geology* 6, 617–638.
- Mackinnon P., Fueten F. & Robin P.Y.F. 1997. A fracture model for quartz ribbons in straight gneisses. *Journal of Structural Geology* 19, 1–14.
- Mancktelow N.S. 1987. Atypical textures in quartz veins from the Simplon Fault Zone. *Journal of Structural Geology* 9, 995–1005.
- Nicolas A. & Poirier J.P. 1976. *Crystalline plasticity and solid state flow in metamorphic rocks*. London: Wiley.
- Passchier C.W. & Trouw R.A.J. 2005. *Microtectonics*. 2nd edn. Berlin: Springer.
- Pennacchioni G., Menegon L., Leiss B., Nestola F. & Bromiley G. 2010. Development of crystallographic preferred orientation and microstructure during plastic deformation of natural coarse-grained quartz veins. *Journal of Geophysical Research—Solid Earth* 115, B12405, doi: <http://dx.doi.org/10.1029/2010JB007674>
- Price G.P. 1985. Preferred orientations in quartzites. In H.R. Wenk (ed.): *Preferred orientation in deformed metals and rocks: an introduction to modern texture analysis*. Pp. 385–406. Orlando, FL: Academic Press.
- Pryer L.L. 1993. Microstructures in feldspar from a major crustal thrust zone: the Grenville Front, Ontario, Canada. *Journal of Structural Geology* 15, 21–36.
- Sander B. 1950. *Einf  hrung in die Gef  gekunde der geologischen K  rper II. Die Korngef  gekunde. (Introduction to fabric analysis of geological bodies II. The fabric of mineral grains.)* Vienna: Springer.

- Schaeben H. & Siemes H. 1996. Determination and interpretation of preferred orientation with texture goniometry: an application of indicators to maximum entropy pole to orientation-density inversion. *Mathematical Geology* 28, 169–201.
- Schmid S.M. & Casey M. 1986. Complete fabric analysis of some commonly observed quartz c-axis patterns. *Geophysical Monographs* 36, 263–286.
- Schulze P. 1992. *Petrogenese des metamorphen Grundgebirges der zentralen Heimefrontfjella (westliches Dronning Maud Land/Antarktis)*. (Petrogenesis of the metamorphic basement complex of the central Heimefrontfjella mountains [western Dronning Maud Land/Antarctica].) *Berichte zur Polarforschung* 117. Bremerhaven: Alfred Wegener Institute.
- Stipp M., Stünitz H., Heilbronner R. & Schmid S.M. 2002. The eastern Tonale fault zone: a “natural laboratory” for crystal plastic deformation of quartz over a temperature range from 250 to 700°C. *Journal of Structural Geology* 24, 1861–1884.
- Tikoff B. & Teyssier C. 1994. Strain modeling of displacement-field partitioning in transpressional orogens. *Journal of Structural Geology* 16, 1575–1588.
- Toy V.G., Prior D.J. & Norris R.J. 2008. Quartz fabrics in the Alpine Fault mylonites: influence of pre-existing preferred orientations on fabric development during progressive uplift. *Journal of Structural Geology* 30, 602–621.
- Tullis J.A., Christie J.M. & Griggs D.T. 1973. Microstructures and preferred orientations of experimentally deformed quartzites. *GSA Bulletin* 84, 297–314.
- White S. 1976. The effects of strain on the microstructures, fabrics, and deformation mechanisms in quartzites. *Philosophical Transactions Royal Society London A* 283, 69–86.